Available online at www.sciencedirect.com
SCIENCE DIRECT®
International Journal of Heat and Mass Transfer 48 (2005) 1096–1106
International Journal of HEAT and MASS TRANSFER
www.elsevier.com/locate/ijhmt

Sudden or smooth transitions in porous media natural convection

Johnathan J. Vadasz [a,*], Joseph E.A. Roy-Aikins [a], Peter Vadasz [b,1]

[a] Department of Mechanical Engineering, University of KZ-Natal, Private Bag X54001, Durban 4000, South Africa
[b] Department of Mechanical Engineering, Northern Arizona University, P.O. Box 15600, Flagstaff, AZ 86011-5600, USA

Received 29 March 2004; received in revised form 15 September 2004
Available online 8 December 2004

Abstract

In porous media isothermal flow a transition from the Darcy regime, via an inertia dominated regime, towards turbulence is anticipated. In porous medium natural convection the transition to turbulence follows a different route. The first transition from a motionless-conduction regime to steady natural convection is followed by a direct second transition to a non-steady (time dependent) and non-periodic regime (referred to as weak turbulent), prior to the amplitude of the convection reaching such large values as to involve inertial, non-Darcy effects. The latter is due to an additional non-linear interaction that appears in natural convection as a result of the coupling between the equations governing the fluid flow and the energy equation. The present paper deals with identifying whether the transitions are sudden or possibly smooth. The latter is accomplished by using a truncated Galerkin representation of the natural convection problem in a porous layer heated from below (an extended Darcy model) leading to the familiar Lorenz equations for the evolution of the convection amplitudes with time. Two different formulations (named the "original" and the "modified" systems) are being used in an anticipation to obtaining a smooth transition in the form of an imperfect bifurcation from the "modified" system formulation. The results show that the transition remains sudden and the accuracy of the "modified" system results is being tested in comparison with the "original" system showing a sufficiently high degree of accuracy.

Keywords: Weak turbulence; Natural convection; Porous media; Chaos

1. Introduction

In porous medium natural convection the transition to turbulence follows the following route. The first transition is from a motionless-conduction regime to steady natural convection. This is followed by a direct second transition to a non-steady (time dependent) and non-periodic regime (referred to as weak turbulent), prior to the amplitude of the convection reaching such large values as to involve inertial, non-Darcy effects. The latter is due to an additional non-linear interaction that appears in natural convection as a result of the coupling between the equations governing the fluid flow and the energy equation.

* Corresponding author. Tel.: +27 31 260 7379; fax: +27 31 260 7002.
E-mail addresses: vadaszJ@ukzn.ac.za (J.J. Vadasz), peter.vadasz@nau.edu (P. Vadasz).
[1] Tel.: +1 928 523 5843; fax: +1 928 523 8951.

0017-9310/$ - see front matter © 2004 Elsevier Ltd. All rights reserved.
doi:10.1016/j.ijheatmasstransfer.2004.09.039

Nomenclature

Da	Darcy number, defined by k_*/H_*^2
H_*	the height of the layer
H	the front aspect ratio of the porous layer, equals H_*/L_*
k_*	permeability of the porous domain
L_*	the length of the porous layer
L	reciprocal of the front aspect ratio, equals $1/H = L_*/H_*$
M_f	ratio of the fluid and the porous domain heat capacities
p	reduced pressure (dimensionless).
Pr	Prandtl number, equals v_*/α_{e*}
Ra	porous media gravity related Rayleigh number, equals $\beta_*\Delta T_C g_* H_* k_* M_f/\alpha_{e*} v_*$
Ra_0	critical Rayleigh number value for loss of stability of the steady convection solution
R	scaled Rayleigh number, equals $Ra/4\pi^2$
R_0	critical value of R for the loss of linear stability of the steady convection solution
r	absolute value of the complex amplitude
r_0	initial condition of r
t	time
T	dimensionless temperature, equals $(T_* - T_C)/(T_H - T_C)$.
T_C	coldest wall temperature
T_H	hottest wall temperature
u	horizontal x component of the filtration velocity
v	horizontal y component of the filtration velocity
w	vertical component of the filtration velocity
x	horizontal length co-ordinate
X	amplitude of convection flow defined in Eq. (6)
y	horizontal width co-ordinate
Y	amplitude of convection temperature defined in Eq. (7)
z	vertical co-ordinate
Z	amplitude of convection defined in Eq. (7)

Greek symbols

α	a parameter related to the time derivative term in Darcy's equation
α_{e_*}	effective thermal diffusivity
β_*	thermal expansion coefficient
ε	asymptotic expansion parameter, see text following Eq. (17)
ϕ	porosity
χ	dimensionless group, equals $\phi Pr/Da$
v_*	fluid's kinematic viscosity
μ_*	fluid's dynamic viscosity
ψ	stream function
ΔT_C	characteristic temperature difference
τ	long time scale
θ	the phase of the complex amplitude

Subscripts

*	dimensional values
t	transitional values
cr	critical values

Superscript

*	complex conjugate

Modeling the weak turbulent regime for natural convection in a fluid saturated porous layer is known to be extremely sensitive to initial conditions. The question of compatibility of the initial conditions between the computational and analytical (weak non-linear) solutions arises in particular in connection with the prediction of the transition point. Vadasz and Olek [1,2] demonstrated by using a computational method of solution (Adomian's decomposition method [3–5]) that the transition from steady to chaotic (weak-turbulent) convection in porous media can be recovered from a truncated Galerkin approximation which yields a system that is equivalent to the familiar Lorenz equations (Lorenz [6], and Sparrow [7]). In particular it was noticed that the transition to chaos occurs at a particular subcritical value of Rayleigh number. Here, the term "sub-critical" is used in the context of the transition from steady convection to a non-periodic state, typically referred to as chaotic, and the critical value of the Rayleigh number is the value at which this transition to chaos is predicted by the linear stability analysis of the convective steady state solutions. The problem that the linear stability analysis reveals that the transition occurs at Rayleigh number values substantially smaller than those obtained by accurate numerical solutions (or by experimental results of an equivalent system that is governed by the same set of Lorenz equations, Yuen and Bau [8] and Wang et al. [9]) and in some cases at values smaller by 50% was addressed by Vadasz [10]. The latter showed that an analytical, weak non-linear, method of solution to this problem, can provide accurate transition values via a correction to the linear stability results. In addition, Vadasz [10] revealed a mechanism for the well known Hysteresis phenomenon in the transition from steady to chaotic convection and backwards. The transition from the steady to the chaotic solution occurs via a subcritical Hopf bifurcation (see Sparrow [7], Yuen and Bau [8] and Wang et al. [9], Vadasz [10,11]) and is asso-

ciated with a homoclinic explosion when the trajectory which originally moves around one steady convective solution (fixed point) departs towards the other fixed point (trajectory here is used in the mathematical sense and not the fluid mechanics sense of a particle trajectory). In order for the analytical solution to provide results that are equivalent to the computational solution, used by Vadasz and Olek [1,2], a compatibility condition for their initial conditions needed to be imposed (see Vadasz [11]). This condition constrained the set of possible initial conditions to a particular group that followed some derived relationships. The application of this method to evaluate the heat transfer coefficient in porous media convection was presented by Vadasz [12] and additional effects were considered by Vadasz [13,14] and Vadasz and Olek [15]. Similar studies of the corresponding convection problem in a pure fluid (non-porous domain) were presented by Vadasz [16,17] and in a rotating porous layer by Vadasz and Olek [18].

The present paper focuses on a different, although equivalent formulation, of the problem in order to obtain more insight into the form of the transition from steady to weak turbulent convection. Analytical work is combined here with computational results in order to further the understanding of this transition. In the first instance our aim here is to demonstrate the equivalence between the two equivalent formulations of the problem at hand and use it to investigate whether the transition is sudden or smooth.

2. Problem formulation and reduced set of equations

A fluid saturated porous layer subject to gravity and heated from below as presented in Fig. 1 is considered. A Cartesian co-ordinate system is used such that the vertical axis z is collinear with gravity, i.e. $\hat{\boldsymbol{e}}_g = -\hat{\boldsymbol{e}}_z$. The time derivative term is not neglected in Darcy's equation in order to investigate the effect of high frequencies associated with small time scales on the results. Weak turbulence is certainly linked to a wide spectrum of frequencies from very low to extremely large. To capture this effect one cannot disregard time derivative terms on the grounds of a small coefficient only. The latter was introduced and discussed by Vadasz [19], and adopted by Straughan [20]. Other than that, Darcy's law is assumed to govern the fluid flow while the Boussinesq approximation is applied for the effects of density variations. Under these conditions the following dimensionless set of governing equations applies (see Pop et al. [21] for the corresponding dimensional form excluding the time derivative term in Eq. (2))

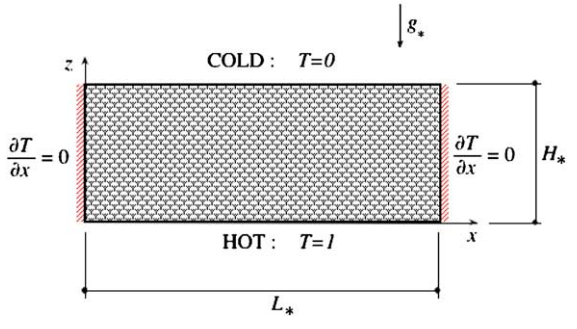

Fig. 1. A fluid saturated porous layer heated from below.

$$\nabla \cdot \boldsymbol{q} = 0 \tag{1}$$

$$\left[\frac{1}{\chi}\frac{\partial}{\partial \hat{t}} + 1\right]\boldsymbol{q} = -\nabla p + RaT\hat{\boldsymbol{e}}_z \tag{2}$$

$$\frac{\partial T}{\partial \hat{t}} + \boldsymbol{q}\cdot\nabla T = \nabla^2 T \tag{3}$$

Eqs. (1)–(3) are presented in a dimensionless form. The values $\alpha_{e*}/H_* M_f$, $\mu_*\alpha_{e*}/k_* M_f$, and $\Delta T_C = (T_H - T_C)$ are used to scale the filtration velocity components (u_*, v_*, w_*), pressure (p_*), and temperature variations ($T_* - T_C$), respectively, where α_{e*} is the effective thermal diffusivity, μ_* is fluid's viscosity, k_* is the permeability of the porous matrix and M_f is the ratio between the heat capacity of the fluid and the effective heat capacity of the porous domain. The height of the layer H_* was used for scaling the variables x_*, y_*, z_* and H_*^2/α_{e*} for scaling the time t_*. Accordingly, $x = x_*/H_*$, $y = y_*/H_*$ and $z = z_*/H_*$, and $t = t_*\alpha_{e*}/H_*^2$. In Eq. (2) Ra is the gravity related Darcy–Rayleigh number defined in the form $Ra = \beta_*\Delta T_c g_* H_* k_* M_f/\alpha_{e*}\nu_*$, where β_* is the thermal expansion coefficient, g_* is the gravity acceleration, ϕ is the porosity, M_f is a ratio between the heat capacity of the fluid and the effective heat capacity of the porous domain and ν_* is the kinematic viscosity of the fluid.

The time derivative term was included in Darcy's Eq. (2), where χ is a dimensionless group which is defined in the form $\chi = \phi Pr/Da$. In traditional applications of transport phenomena in porous media typical values of χ are quite big, a fact that provides a justification for the neglect of the time derivative term in Darcy's equation. However, when wave phenomena are of interest the time derivative term is expected to be included in order to prevent the reduction of the order of the system in the time domain.

As all the boundaries are rigid the solution must follow the impermeability conditions there, i.e. $\boldsymbol{q}\cdot\hat{\boldsymbol{e}}_n = 0$ on the boundaries, where $\hat{\boldsymbol{e}}_n$ is a unit vector normal to the boundary. The temperature boundary conditions are $T = 1$ at $z = 0$, $T = 0$ at $z = 1$ and $\nabla T\cdot\hat{\boldsymbol{e}}_n = 0$ on all other walls representing the insulation condition on these walls.

For convective rolls having axes parallel to the shorter dimension (i.e. y) $v = 0$, and the governing

equations can be presented in terms of a stream function defined by $u = \partial\psi/\partial z$ and $w = -\partial\psi/\partial x$, which upon substitution into Eqs. (1) and (2) yields

$$\left[\frac{1}{\chi}\frac{\partial}{\partial \hat{t}} + 1\right]\left[\frac{\partial^2\psi}{\partial x^2} + \frac{\partial^2\psi}{\partial z^2}\right] = -Ra\frac{\partial T}{\partial x} \tag{4}$$

$$\frac{\partial T}{\partial \hat{t}} + \frac{\partial\psi}{\partial z}\frac{\partial T}{\partial x} - \frac{\partial\psi}{\partial x}\frac{\partial T}{\partial z} = \frac{\partial^2 T}{\partial x^2} + \frac{\partial^2 T}{\partial z^2} \tag{5}$$

where the boundary conditions for the stream function are $\psi = 0$ on the horizontal boundaries. Here T is the dimensionless temperature and $\hat{t}$ is the dimensionless time.

To obtain the complete solution to the non-linear coupled system of partial differential Eqs. (4) and (5) we represent the stream function and temperature in the form

$$\psi = -\frac{2L\sqrt{2\gamma(R-1)}}{\gamma}X(t)\sin(\pi x)\sin(\pi z) \tag{6}$$

$$T = 1 - z + \frac{2\sqrt{2\gamma(R-1)}}{\pi R}Y(t)\cos(\pi x)\sin(\pi z) - \frac{(R-1)}{\pi R}Z(t)\sin(2\pi z) \tag{7}$$

where $R = \gamma^2 Ra/\pi^2$ is the scaled Rayleigh number, $\gamma = L^2/(L^2+1)$, $L = L_*/H_*$ is the reciprocal of the layer's aspect ratio, and the time was rescaled in the form $t = (L^2+1)\pi^2\hat{t}/L^2$. This representation is equivalent to a Galerkin expansion of the solution in both x and z directions, truncated when $i + j = 2$, where i is the Galerkin summation index in the x direction and j is the Galerkin summation index in the z direction. It may be interesting to note that applying a weak non-linear method of solution directly to Eqs. (4) and (5) produces a solution that includes only the first spatial modes in both ψ and T. Therefore the representation of the solution in the form (6) and (7) is an extension of the weak non-linear solution by including one more spatial mode. Substituting (6) and (7) into the Eqs. (4) and (5), multiplying the equations by the orthogonal eigenfunctions corresponding to (4) and (5) and integrating them over the domain, i.e. $\int_0^1 dx \int_0^1 dz(\cdot)$, yields a set of three ordinary differential equations for the time evolution of the amplitudes in the form

$$\dot{X} = \alpha(Y - X) \tag{8}$$

$$\dot{Y} = RX - Y - (R-1)XZ \tag{9}$$

$$\dot{Z} = 4\gamma(XY - Z) \tag{10}$$

subject to the initial conditions $X = X_0$, $Y = Y_0$, $Z = Z_0$, where $\alpha = \gamma\chi/\pi^2$, and the dots $(\cdot)$ denote time derivatives $d(\,)/dt$. Eqs. (8)–(10) are equivalent to Lorenz equations (Lorenz [6], Sparrow [7]), which are satisfied by the stationary (or fixed) point corresponding to the motionless-conduction solution $X_S = Y_S = Z_S = 0$, by the stationary points corresponding to the steady convective solutions $X_S = Y_S = \pm 1$ and $Z_S = 1$, and by chaotic solutions. The linear stability of the fixed point associated with the motionless solution ($X_S = Y_S = Z_S = 0$) is obtained by investigating the growth or decay of small perturbations around the motionless solution ($X_S = Y_S = Z_S = 0$) that have the form $e^{\sigma t}$. Their stability is therefore controlled by the zeros of the following characteristic polynomial equation for the eigenvalues, σ_i ($i = 1, 2, 3$)

$$(4\gamma + \sigma)[\alpha R - (\alpha + \sigma)(1 + \sigma)] = 0 \tag{11}$$

The first eigenvalue $\sigma_1 = -4\gamma$ is always negative because $\gamma = L^2/(L^2+1) > 0$ causing the small perturbations to decay. The other two eigenvalues are always real and given by

$$\sigma_2 = \frac{1}{2}\left[-(\alpha+1) + \sqrt{(\alpha+1)^2 + 4\alpha(R-1)}\right] \tag{12a}$$

$$\sigma_3 = \frac{1}{2}\left[-(\alpha+1) - \sqrt{(\alpha+1)^2 + 4\alpha(R-1)}\right] \tag{12b}$$

Note from Eq. (12) that the eigenvalue σ_3 is also always negative because $\alpha = \gamma\chi/\pi^2 > 0$, causing the perturbations to decay. On the other hand the sign of σ_2 provides the stability condition for the motionless solution in the form $\sigma_2 < 0 \iff R < 1$, because a value of $R > 1$ causes the term under the square-root in (12a) to be larger than $(\alpha+1)^2$ leading to the square brackets and therefore σ_2 to become positive. A positive value of $\sigma_2 > 0$ causes the perturbations to grow indicating the instability of the motionless solution $X_S = Y_S = Z_S = 0$. Alternatively, when $R < 1$ the term under the square-root in (12a) is smaller than $(\alpha+1)^2$ leading to the square brackets and therefore σ_2 to be negative, resulting in the decay of the perturbation and therefore to a stable motionless solution. Therefore the critical value of R, where the motionless solution loses stability and the steady convection solution (expressed by the other two fixed points) takes over, is obtained as $R = 1$, which for a porous layer of infinite horizontal extent ($L \to \infty$) being associated with $\gamma = \lim_{L\to\infty}[L^2/(L^2+1)] = 0.5$, corresponds to $Ra_{cr} = 4\pi^2$, recovering the familiar stability condition of the Horton–Rodgers–Lapwood convection. A similar linear stability analysis of the steady convection solutions $X_S = Y_S = \pm 1$ and $Z_S = 1$, indicates that the latter are stable when $1 < R < R_0$, where $R_0 = \alpha(\alpha + 4\gamma + 3)/(\alpha - 4\gamma - 1)$. One may conclude that the motionless solution $X_S = Y_S = Z_S = 0$ is stable when $R < 1$, the steady convective solutions $X_S = Y_S = \pm 1$ and $Z_S = 1$ are stable when $1 < R < R_0$, and non-steady, non-periodic solutions (chaotic) may appear for values of $R > R_0$. The transition from the steady to the chaotic solution occurs via a subcritical Hopf bifurcation (see Sparrow [7], Yuen and Bau [8], Wang et al. [9], Vadasz

[10–12]) and is associated with a homoclinic explosion when the trajectory that originally moves around one steady convective solution (fixed point) departs towards the other fixed point.

The problem formulation used here is slightly different than Eqs. (8)–(10) although fully equivalent. It essentially consists of introducing the initial conditions into the equations by using the transformation

$$\widetilde{X} = X - X_0; \quad \widetilde{Y} = Y - Y_0; \quad \widetilde{Z} = Z - Z_0 \tag{13}$$

which produces the following set of equations

$$\dot{\widetilde{X}} = \alpha(\widetilde{Y} - \widetilde{X}) - \alpha(Y_0 - X_0) \tag{14}$$

$$\dot{\widetilde{Y}} = [R - (R-1)Z_0]\widetilde{X} - \widetilde{Y} - (R-1)X_0\widetilde{Z} - (R-1)\widetilde{X}\widetilde{Z} - RX_0 - RY_0 - (R-1)X_0Z_0 \tag{15}$$

$$\dot{\widetilde{Z}} = 4\gamma(\widetilde{X}\widetilde{Y} - \widetilde{Z} + X_0\widetilde{Y} + Y_0\widetilde{X} + X_0Y_0 - Z_0) \tag{16}$$

subject to the initial conditions $\widetilde{X}_0 = \widetilde{Y}_0 = \widetilde{Z}_0 = 0$.

The system of Eqs. (8)–(10) was solved computationally via the Adomian decomposition method [3–5] and its results were compared with the corresponding numerical solution obtained from system (14)–(16) by applying a fifth and sixth order Runge–Kutta–Verner method from the IMSL Library (DIVPRK) [22]. In addition both systems were solved analytically via the weak non-linear method by using an asymptotic expansion around the value of $R = R_0$, i.e. around the point where the convective fixed points loose stability in the linear sense. The computational as well as the numerical results indicate that the point of transition from steady to chaotic solution is detected at a sub-critical value of $R_t < R_0$, in some cases the transition occurs at values of R_t as small as $R_0/2$. The latter deviation is explained by using the analytical weak non-linear method of solution to provide a correction to the linear stability results in the form of an analytical closed form expression (see Eq. (25) in what follows). It is therefore a major objective of this paper to use the analytical relationship for this transition value of $R = R_t$, to be derived and presented in Eq. (25), and compare it with the corresponding values obtained computationally. The anticipation was to establish whether the perfect Hopf bifurcation renders itself imperfect due to the introduction of the initial conditions into the equations.

3. Analytical method of solution

The analytical solution to the problem is evaluated via a weak non-linear analysis by using an expansion around the point where the convective stationary solutions loose linear stability. The stationary (fixed) points of the system (8)–(10) are the convective solutions $X_S = Y_S = \pm 1$, $Z_S = 1$ and the motionless solution $X_S = Y_S = Z_S = 0$ (referred to as the origin). The expansion around the motionless stationary solution yields the familiar results of a pitchfork bifurcation from a motionless state to convection at $R = 1$. We expand now the dependent variables around the convection stationary points in the form

$$[X, Y, Z] = [X_S, Y_S, Z_S] + \varepsilon[X_1, Y_1, Z_1] + \varepsilon^2[X_2, Y_2, Z_2] + \varepsilon^3[X_3, Y_3, Z_3] + \cdots \tag{17}$$

We also expand R in a finite series of the form $R = R_0(1 + \varepsilon^2)$ which now defines the small expansion parameter as $\varepsilon^2 = (R - R_0)/R_0$, where R_0 is the value of R where the stationary convective solutions lose their stability in the linear sense (see Vadasz and Olek [1,2]). Therefore the present weak non-linear analysis is expected to be restricted to initial conditions sufficiently close to *any one* of the convective fixed points. Introducing a long time scale $\tau = \varepsilon^2 t$ and replacing the time derivatives in Eqs. (8)–(10) with $\mathrm{d}/\mathrm{d}t \to \mathrm{d}/\mathrm{d}t + \varepsilon^2\mathrm{d}/\mathrm{d}\tau$, yields a hierarchy of ordinary differential equations at the different orders. The solutions to order $O(\varepsilon)$ have the form:

$$X_1 = a_1 e^{\sigma_r + i\sigma_0 t} + a_1^* e^{\sigma_r - i\sigma_0 t} + a_{13} e^{\sigma_3 t} \tag{18}$$

$$Y_1 = b_1 e^{\sigma_r + i\sigma_0 t} + b_1^* e^{\sigma_r - i\sigma_0 t} + b_{13} e^{\sigma_3 t} \tag{19}$$

$$Z_1 = c_1 e^{\sigma_r + i\sigma_0 t} + c_1^* e^{\sigma_r - i\sigma_0 t} + c_{13} e^{\sigma_3 t} \tag{20}$$

where $\sigma_1 = \sigma_r + i\sigma_0$, $\sigma_2 = \sigma_r - i\sigma_0$ and σ_3 are the three eigenvalues of the system (8)–(10) linearised around R_0. It turns out that the first two, σ_1 and σ_2 are a pair of complex conjugate eigenvalues, while the third one is real and negative, i.e. $\sigma_3 < 0$ and real. At marginal stability, i.e. at $R = R_0$, the real part of the complex eigenvalues is zero. Therefore, at order $O(\varepsilon)$ one can set the argument of the exponents in Eq. (18)–(20) to $\sigma_1 = i\sigma_0$ and $\sigma_2 = -i\sigma_0$, by substituting $\sigma_r = 0$. What typically follows when using the weak non-linear method of solution is the neglect of the decaying term $a_{13}e^{\sigma_3 t}$ from the solution. This term does not bring any contribution to the post-transient solution. However, while indeed this term vanishes at the post-transient state, its inclusion in the solution becomes essential in order to provide a relationship between the initial conditions in the analytical solution and the computational one. The coefficients $a_1(\tau)$, $a_1^*(\tau), b_1(\tau), b_1^*(\tau)c_1(\tau)$ and $c_1^*(\tau)$ are allowed to vary over the long time scale τ. By substituting the solutions (15), (19) and (20) into the linearised form of Eqs. (8)–(10), that apply at order $O(\varepsilon)$ (see Vadasz [10] for details), one obtains the following relationships between these coefficients

$$b_1 = \frac{(\alpha + i\sigma_0)}{\alpha} a_1; \quad b_1^* = \frac{(\alpha - i\sigma_0)}{\alpha} a_1^*; \quad b_{13} = \frac{(\sigma_3 + \alpha)}{\alpha} a_{13} \tag{21}$$

$$c_1 = \frac{\sigma_0[\sigma_0 - \mathrm{i}(\alpha+1)]}{\alpha(R_0-1)}a_1;$$
$$c_1^* = \frac{\sigma_0[\sigma_0 + \mathrm{i}(\alpha+1)]}{\alpha(R_0-1)}a_1^*;$$
$$c_{13} = \frac{-\sigma_3[\sigma_3+\alpha+1]}{\alpha(R_0-1)}a_{13} \tag{22}$$

The values of σ_0, R_0 and σ_3 corresponding to $\sigma_r = 0$ are also obtained in the form $\sigma_0^2 = 8\alpha\gamma(\alpha+1)/(\alpha-4\gamma-1)$, $R_0 = \alpha(\alpha+4\gamma+3)/(\alpha-4\gamma-1)$ and $\sigma_3 = -(\alpha+4\gamma+1)$.

A solvability condition is obtained at order $O(\varepsilon^3)$ in order to prevent terms of the form $e^{i\sigma_0 t}$ and $e^{-i\sigma_0 t}$ on the right hand side of the $O(\varepsilon^3)$ equations to resonate the homogeneous operator, hence forcing secular solutions of the form $te^{i\sigma_0 t}$ and $te^{-i\sigma_0 t}$ that are not bounded as $t \to \infty$. Hence, the coefficients of these secular terms must vanish, a requirement which provides a constraint on the amplitudes at order $O(\varepsilon)$ in the form of an amplitude equation

$$\frac{\mathrm{d}r}{\mathrm{d}t} = s[\xi - r^2]r \tag{23}$$

subject to the initial condition $t = 0$: $r = r_0$, where the $O(\varepsilon)$ complex amplitude was presented in the form

$$a = \varepsilon a_1 = re^{i\theta} \quad a^* = \varepsilon a_1^* = re^{-i\theta} \tag{24}$$

with $aa^* = r^2$, $s = \varphi/\beta$ and $\xi = \varepsilon^2/\varphi$, where φ and β are parameters that depend on the value of α. For $\alpha = 5$, corresponding to $\chi \cong 98.7$ and consistent with the present study $\varphi = -2.4$, $\beta = 0.403226$ (the value of φ was found to be negative over a very wide band of α values that are compatible with the Hopf bifurcation), and the following critical values apply $R_0 = 25$ and $\sigma_0 = \sqrt{60}$. The transient solution to Eq. (23) identifies the transition from steady to weak-turbulent convection (see Vadasz [10–12] for details) in terms of ξ and r_0^2 in the form $r_0^2 > \xi$. Transforming the condition for this transition to occur, from $r_0^2 > \xi$, to the original physical parameters of the system by substituting the definition of ξ and ε^2 one can observe that there is a value of $R < R_0$, say R_t, beyond which the transition occurs, which can be expressed in the form

$$R_t = R_0(1 - \mid \varphi \mid r_0^2) \tag{25}$$

where the minus sign and the absolute value of φ appear in order to show explicitly that $\varphi < 0$. If $R < R_t$ the solution decays, spiraling towards the corresponding fixed point, at $R = R_t$ we expect a solitary limit cycle solution, and beyond this transitional value of R, i.e. $R > R_t$, the solution moves away from this fixed point, towards a possible chaotic solution. It is important to stress that for any initial condition r_0^2, which we choose, we can find a value of $R < R_0$ which satisfies Eq. (25). At that value of R we expect to obtain a limit cycle solution and beyond it a possible chaotic solution.

Since in the computational/numerical solutions we use as initial conditions X_0, Y_0 and Z_0 while the analytical solution provides the transition point R_t in terms of r_0 a compatibility relationship between X_0, Y_0 and Z_0 and r_0 is required (Vadasz [11]). For the particular case when $X_0 = Y_0 = Z_0$ the relationship is simple and is presented in the form

$$\tan(\theta_0) = \frac{\sigma_3[\sigma_0^2 - \alpha(R_0-1)]}{\sigma_0[\sigma_3^2 + \alpha(R_0-1)]} \quad \text{for } \widehat{X}_0 = \widehat{Y}_0 = \widehat{Z}_0 \tag{26}$$

$$r_0 = \frac{\sigma_3}{2[\sigma_3\cos(\theta_0) + \sigma_0\sin(\theta_0)]}\widetilde{X}_0 \quad \text{for } \widehat{X}_0 = \widehat{Y}_0 = \widehat{Z}_0 \tag{27}$$

where $\widehat{X}_0 = X_0 - 1$, $\widehat{Y}_0 = Y_0 - 1$ and $\widehat{Z}_0 = Z_0 - 1$.

A similar analytical method was attempted for the slightly modified (transformed) but equivalent system (14)–(16). It was anticipated that the amplitude equation for the modified formulation takes the form

$$\frac{\mathrm{d}r}{\mathrm{d}t} = s[\xi - r^2]r + \eta \tag{28}$$

where $\eta(r_0)$ is a parameter that was expected to depend on initial conditions. Eq. (28) suggests the existence of an "imperfect Hopf bifurcation", that might probably lead to a smooth rather than a sudden transition, depending on the initial conditions. The convective fixed

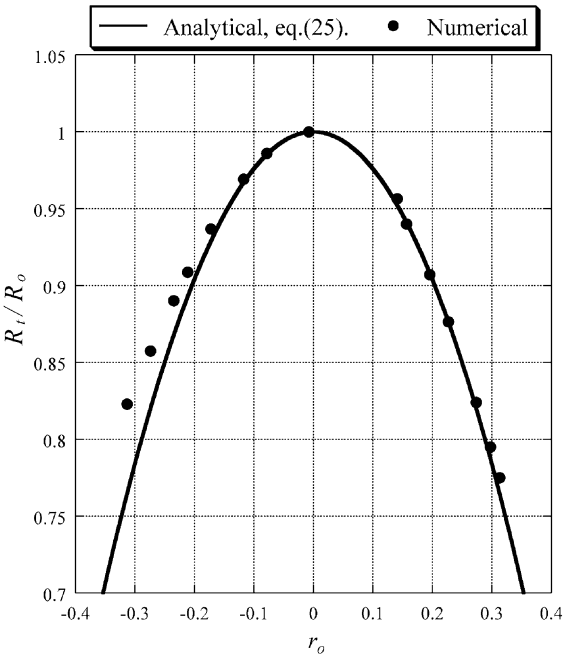

Fig. 2. Transitional sub-critical values of Rayleigh number in terms of R_t/R_0 as a function of the initial conditions r_0. Comparison between the analytical weak non-linear solution expressed by Eq. (25) (–), and the numerical results (●).

points of the modified system (14)–(16) were evaluated as $\widetilde{X}_S = \pm 1 - X_0$, $\widetilde{Y}_S = \pm 1 - Y_0$, and $\widetilde{Z}_S = 1 - Z_0$, and the corresponding expansion of the modified formulation was similar to Eq. (17) in the form

$$[\widetilde{X}, \widetilde{Y}, \widetilde{Z}] = [\widetilde{X}_S, \widetilde{Y}_S, \widetilde{Z}_S] + \varepsilon[\widetilde{X}_1, \widetilde{Y}_1, \widetilde{Z}_1] + \varepsilon^2[\widetilde{X}_2, \widetilde{Y}_2, \widetilde{Z}_2] + \varepsilon^3[\widetilde{X}_3, \widetilde{Y}_3, \widetilde{Z}_3] + \cdots \quad (29)$$

followed by identical expressions for $R = R_0(1 + \varepsilon^2)$ and $\mathrm{d}/\mathrm{d}t \to \mathrm{d}/\mathrm{d}t + \varepsilon^2 \mathrm{d}/\mathrm{d}\tau$. The only difference between the modified and original systems is the inclusion of the initial conditions into the equations leading to homogeneous initial conditions in the modified system, i.e. $\widetilde{X}_0 = \widetilde{Y}_0 = \widetilde{Z}_0 = 0$. Following the same procedure as for the original system yields a hierarchy of ordinary differential equations at the different orders that includes explicitly the initial conditions as well as the stationary points. When substituting the stationary points $\widetilde{X}_S = \pm 1 - X_0$, $\widetilde{Y}_S = \pm 1 - Y_0$, and $\widetilde{Z}_S = 1 - Z_0$, into the equations at all orders it turns out that the initial conditions disappear from all equations, resulting in equations that are identical to the original system. Therefore, we conclude that the initial conditions affect only the stationary points as well as the compatibility condition between the analytical and computational solutions. The Hopf bifurcation at the transition point remains perfect and the transition point is affected by the initial conditions as presented in the following section.

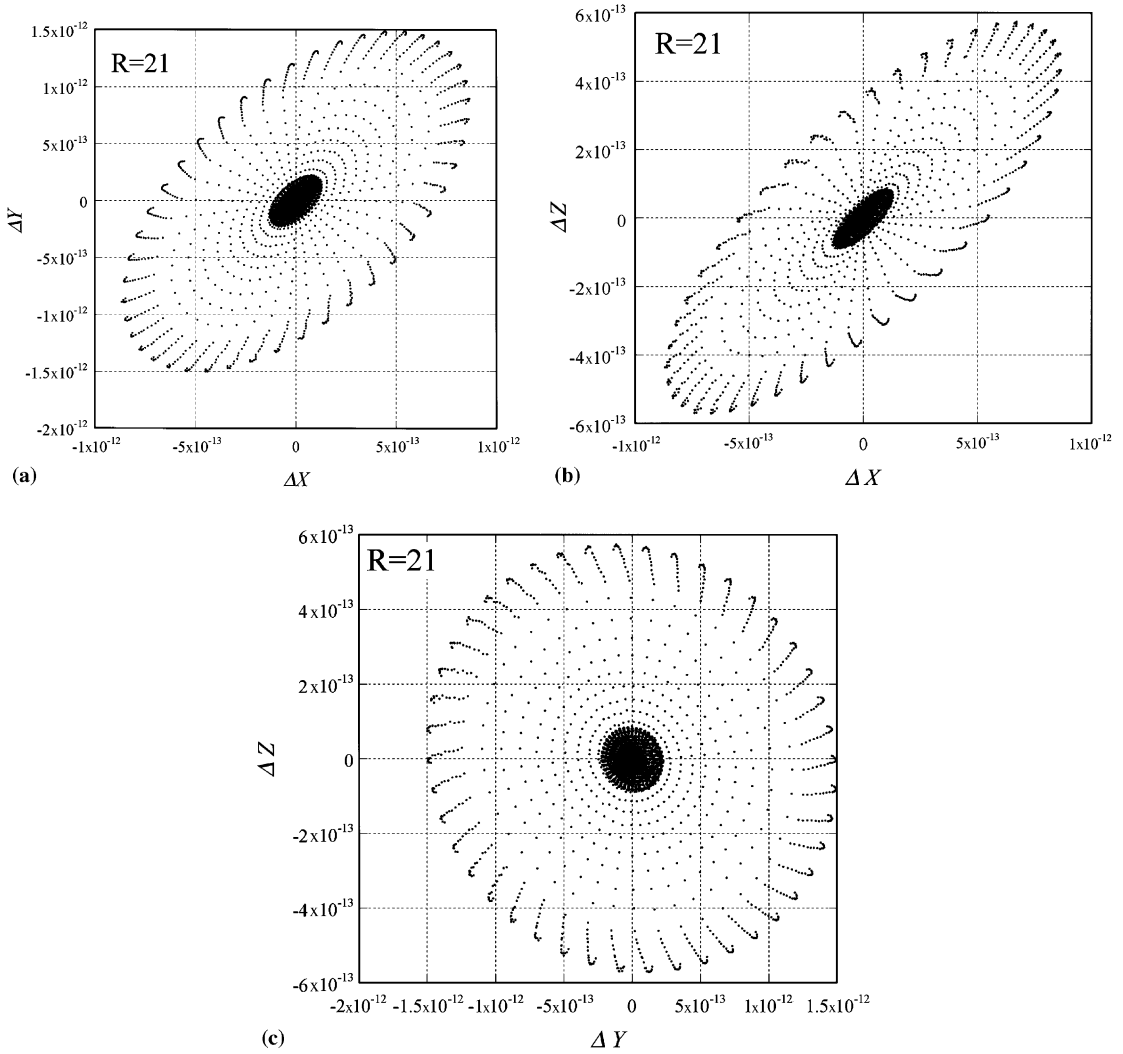

Fig. 3. Trajectory of differences between the "modified system" and "original system" solutions corresponding to $\Delta t = 10^{-3}$, and $R = 21$. (a)–(c) Projection of trajectory's data points on the planes $\Delta Z = 0$, $\Delta Y = 0$ and $\Delta X = 0$, respectively, for $R = 21$.

4. Results and discussion

The objective in the presentation of the following results is to demonstrate the appearance of the transition at particular values of $R = R_t$ and compare the computational and analytical values of R_t. The latter correspond to Eq. (25), for different initial conditions that are consistent with the weak non-linear solution, i.e. they satisfy the compatibility conditions (26) and (27). A sequence of computations was performed in order to evaluate these transitional R values. In all computations the values of $\gamma = 0.5$ and $\alpha = 5$ were used. They yield the following corresponding parameter values $\varphi = -2.4$, $R_0 = 25$, $\sigma_0 = \sqrt{60}$ and $\sigma_3 = -8$. The results are presented in Fig. 2 where the continuous curve represents the analytical solution expressed by Eq. (25) while the different dots represent the numerical results corresponding to different initial conditions. The very good agreement between the analytical and numerical solutions in the neighborhood of the convective fixed point (i.e. $|r_0| \ll 1$) is evident from Fig. 2. Actually for $|r_0| < 0.2$ the numerical and analytical solutions overlap.

As the initial conditions move away from the convective fixed point and the value of $|r_0|$ increases the analytical solution departs from the numerical results, which reconfirms the validity of the weak non-linear solution in the neighborhood of a convective fixed point and its breakdown far away from this point. In addition, the numerical results move apart from each other as well, when $|r_0|$ increases. The reason for this latter departure

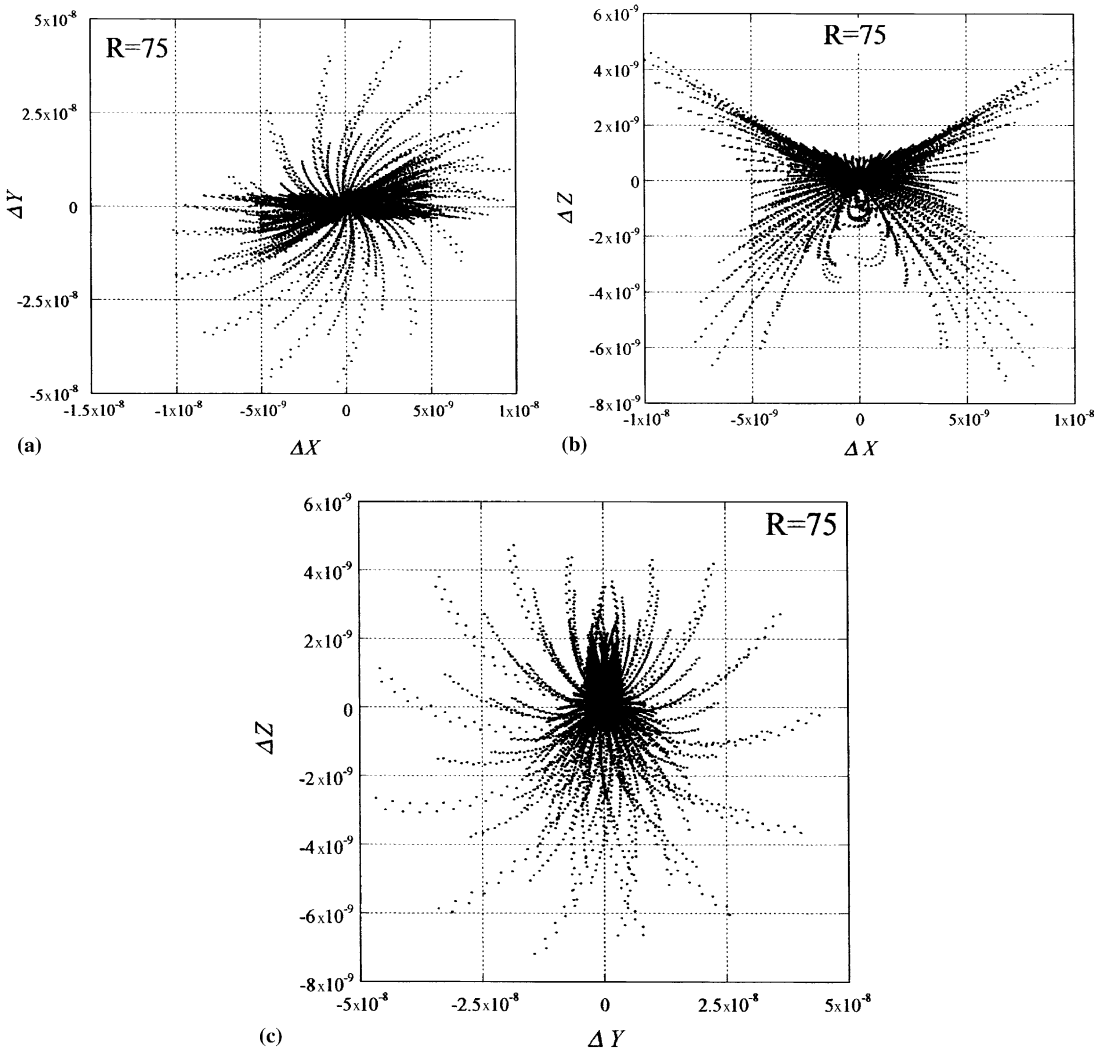

Fig. 4. Trajectory of differences between the "modified system" and "original system" solutions corresponding to $\Delta t = 10^{-3}$, and $R = 75$. (a)–(c) projection of trajectory's data points on the planes $\Delta Z = 0$, $\Delta Y = 0$ and $\Delta X = 0$, respectively.

is the fact that the compatibility of the initial conditions in terms of r_0 was also derived based on the weak non-linear solution at order $O(\varepsilon)$. Therefore, as the latter solution loses accuracy when $|r_0|$ increases, the compatibility conditions lose accuracy as well. The departure between the numerical results and the analytical ones is clearly not symmetrical with respect to $r_0 = 0$. While the $O(\varepsilon)$ weak non-linear solution is symmetrical with respect to $r_0 = 0$, due to its elliptical shape, there is no reason to expect this symmetry from a numerical solution as one moves away from the fixed point (the symmetry is kept for $|r_0| \ll 1$). Actually in the neighborhood of $|r_0| = 0.5$ one may expect to find the homoclinic orbit. Its shape is by far different than the one of an ellipse (see Vadasz and Olek [15]). Both improvement of accuracy and loss of symmetry are expected if higher order corrections are considered.

The last objective of the present paper is to compare the numerical results obtained from the modified but equivalent formulation of the problem ("modified system"), Eqs. (14)–(16) with the corresponding computational results ("original system"), obtained via the Adomian decomposition method ([3–5]) from Eqs. (8)–(10). The numerical solution to the modified formulation of the problem was accomplished to double precision by using the fifth and sixth order Runge–Kutta–Verner method from the IMSL Library (DIVPRK) [22] up to a desired tolerance for error control specified by the parameter tol. The adopted procedure was to solve each system separately to double precision, and evaluate the difference between the two solutions at all values of t up to $t_{max} = 210$. The final step was plotting this difference in results as projections of the trajectory of differences on the planes $\Delta Z = 0$ ($\Delta Y - \Delta X$ plane), $\Delta Y = 0$

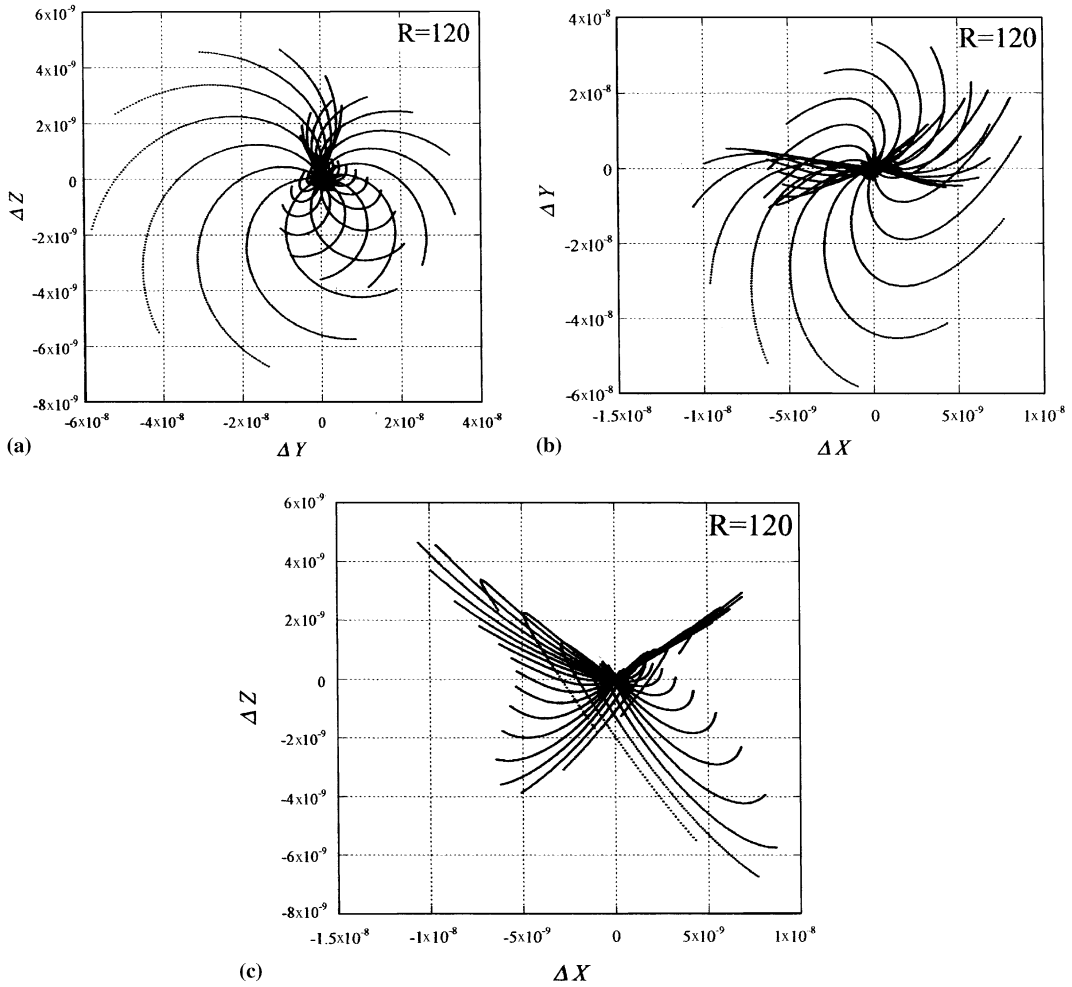

Fig. 5. Trajectory of differences between the "modified system" and "original system" solutions corresponding to $\Delta t = 10^{-3}$, and $R = 120$. (a)–(c) Projection of trajectory's data points on the planes $\Delta Z = 0$, $\Delta Y = 0$ and $\Delta X = 0$, respectively.

($\Delta Z - \Delta X$ plane) and $\Delta X = 0$ ($\Delta Z - \Delta Y$ plane), where $\Delta X = X_{\text{mod.}} - X_{\text{orig.}}$, $\Delta Y = Y_{\text{mod.}} - Y_{\text{orig.}}$ and $\Delta Z = Z_{\text{mod.}} - Z_{\text{orig.}}$. The indices "mod." and "orig." stand for representing the " modified system" and the "original system" results, respectively.

The decomposition method [3–5] provides an analytical solution in the form of an infinite power series. The practical need to evaluate numerical values from the infinite power series suggests its use as an algorithm for the approximation in a sequence of time intervals $\Delta t = t_p - t_{p-1}$. The value of Δt was used as an accuracy control parameter for the "original system", while the value of tol was used as an accuracy control parameter for the "modified system". The results of the comparison between the modified and original systems corresponding to values of $\Delta t = 10^{-3}$ and $\text{tol} = 10^{-12}$, and for $R = 21$, are presented in Fig. 3(a)–(c). From these figures it is evident that the difference between the solutions is of the order of magnitude 10^{-12}, quite close to machine precision accuracy. These results correspond to steady convection, i.e. subcritical conditions ($R = 21$). Naturally, one cannot expect similar results for supercritical conditions when the solution is chaotic, because then two nearby trajectories diverge (at least one their Lyapunov exponents is positive). In order to compare the results between the modified and the original systems at supercritical conditions we use the existence of periodic windows within the chaotic regime and evaluate the comparison at values of R corresponding to these periodic windows. The first wide periodic window appears around $R = 75$ (see Vadasz and Olek [1]). The results of the comparison between the modified and original systems corresponding to $R = 75$ are presented in Fig. 4(a)–(c). From the figure it is evident that the difference between the solutions although larger than the previous case is still quite small, i.e. of an order of magnitude of 10^{-8}. The differences in the results of the "modified" and "original" systems for another periodic regime at $R = 120$ is presented in Fig. 5(a)–(c) in terms of projections of trajectories of differences on the $\Delta Z = 0$ and $\Delta Y = 0$ and $\Delta X = 0$ planes. The figure shows that the difference between the solutions is also of the order of magnitude of 10^{-8}. These results indicate that numerically both systems produce results that are sufficiently accurate to be representative in the comparison with analytical solutions as previously presented. The shapes appearing in the figures in terms of differences are similar and they retain this similarity under scale reduction and magnification.

5. Conclusions

The derivation of a set of modified, but equivalent, system of equations that might reveal the nature of the transition process in the weak turbulent regime was investigated and tested for accuracy. The results show that the numerical solution to the modified system produces results that are sufficiently accurate when compared to the original system. The transition values of the Rayleigh number were compared against analytical predictions revealing again a very good match. The anticipation that the analytical solution of the "modified" system might reveal a smooth rather than a sudden transition from steady convection to weak-turbulence via an imperfect Hopf bifurcation was not fulfilled. The Hopf bifurcation of the "modified" system remained perfect. The transition is therefore sudden.

Acknowledgments

The authors wish to thank the University of KZ-Natal (Westville Campus) for partially supporting this study.

References

[1] P. Vadasz, S. Olek, Weak turbulence and chaos for low Prandtl number gravity driven convection in porous media, Transport Porous Med. 37 (1) (1999) 69–91.
[2] P. Vadasz, S. Olek, Route to chaos for moderate Prandtl number convection in a porous layer heated from below, Transport Porous Med. 41 (2) (2000) 211–239.
[3] G. Adomian, A review of the decomposition method in applied mathematics, J. Math. Anal. Appl. 135 (1988) 501–544.
[4] G. Adomian, Solving Frontier Problems in Physics: The Decomposition Method, Kluwer Academic Publishers, Dordrecht, 1994.
[5] P. Vadasz, S. Olek, Convergence and accuracy of Adomian's decomposition method for the solution of Lorenz equations, Int. J. Heat Mass Transfer 43 (10) (2000) 1715–1734.
[6] E.N. Lorenz, Deterministic non-periodic flows, J. Atmos. Sci. 20 (1963) 130–141.
[7] C. Sparrow, The Lorenz Equations: Bifurcations, Chaos, and Strange Attractors, Springer-Verlag, New York, 1982.
[8] P. Yuen, H.H. Bau, Rendering a subcritical Hopf bifurcation supercritical, J. Fluid Mech. 317 (1996) 91–109.
[9] Y. Wang, J. Singer, H.H. Bau, Controlling chaos in a thermal convection loop, J. Fluid Mech. 237 (1992) 479–498.
[10] P. Vadasz, Local and global transitions to chaos and hysteresis in a porous layer heated from below, Transport Porous Med. 137 (2) (1999) 213–245.
[11] P. Vadasz, Equivalent initial conditions for compatibility between analytical and computational solutions of convection in porous media, Int. J. Non-Linear Mech. 36 (2) (2001) 197–208.
[12] P. Vadasz, Heat transfer regimes and hysteresis in porous media convection, ASME J. Heat Transfer 123 (2001) 145–156.

[13] P. Vadasz, The effect of thermal expansion on porous media convection. Part 1. Thermal expansion solution, Transport Porous Med. 44 (3) (2001) 421–443.
[14] P. Vadasz, The effect of thermal expansion on the transition to chaos in porous media convection. Part 2. Thermal convection solution, Transport Porous Med. 44 (3) (2001) 445–463.
[15] P. Vadasz, S. Olek, Computational recovery of the homoclinic orbit in porous media convection, Int. J. Non-Linear Mech. 34 (6) (1999) 89–93.
[16] P. Vadasz, Subcritical transitions to chaos and hysteresis in a fluid layer heated from below, Int. J. Heat Mass Transfer 43 (5) (1999) 705–724.
[17] P. Vadasz, On the homoclinic orbit for convection in a fluid layer heated from below, Int. J. Heat Mass Transfer 42 (19) (1999) 3557–3561.
[18] P. Vadasz, S. Olek, Transitions and chaos for free convection in a rotating porous layer, Int. J. Heat Mass Transfer 14 (11) (1998) 1417–1435.
[19] P. Vadasz, Coriolis effect on gravity driven convection in a rotating porous layer heated from below, J. Fluid Mech. 376 (1998) 351–375.
[20] B. Straughan, A sharp nonlinear stability threshold in rotating porous convection, Proc. Roy. Soc. Lond. A457 (2001) 87–93.
[21] I. Pop, D.B. Ingham, J.H. Merkin, Transient convection heat transfer in a porous medium: external flows, in: D.B. Ingham, I. Pop (Eds.), Transport Phenomena in Porous Media, Pergamon, Oxford, 1998, pp. 205–231.
[22] IMSL Library, 1991, Fortran Subroutines for Mathematical Applications, Version 2, Houston.